Available online at www.sciencedirect.com
ScienceDirect
Cement and Concrete Research 38 (2008) 312–319
Cement and Concrete Research

# Early-age hydration of fresh concrete monitored by non-contact electrical resistivity measurement

Lianzhen Xiao, Zongjin Li *

*Department of Civil Engineering, the Hong Kong University of Science & Technology, Hong Kong*

Received 25 November 2005; accepted 19 September 2007

**Abstract**

This paper reports the investigations on the early hydration process of fresh concrete using a non-contact electrical resistivity measurement. The bulk resistivity development ($\rho(t)$–$t$ curves) and the pore solution resistivity development ($\rho_0(t)$–$t$ curves) of fresh concrete, with and without fly ash replacement, were obtained for the period from casting to the age of 48 h. The porosity development ($\phi(t)$–$t$ curves) was obtained from the $\rho(t)$–$t$ and $\rho_0(t)$–$t$ evolution curves with the calculated initial porosity and the measured porosity at 1 day by mercury intrusion porosimetry (MIP). The degree of hydration ($\alpha(t)$–$t$) of the cement-based materials was then obtained based on the porosity change with time, which was caused by the increase of hydration products with a lower density as compared to that of the original cement in the hydration system. The comparison of the degree of hydration predicted from the porosities ($\phi(t)$–$t$) and obtained from the experimental measurement of non-evaporable water showed a good agreement of the two.

The setting and hardening behavior of fresh concrete was characterized by the characteristic points on the $\rho(t)$–$t$ and $d\rho(t)/dt$–$t$ curves. The retarded hydration caused by the fly ash incorporation could be identified by the characteristic points.


*Keywords:* Electrical resistivity; Fresh concrete; Porosity; Degree of hydration

## 1. Introduction

Cement-based materials have a complex hydration process and microstructure, varying in time and depending on chemical composition, admixture incorporation and temperature. The degree of hydration describes the process of hydration, and directly relates to the fraction of the hydration products or porosity in a hydration system that governs the properties of cement-based materials. There are many methods to estimate the degree of hydration of cement, such as calorimetry, chemically bonded water, X-ray diffraction and image analysis. However, different methods give different results for the degree of hydration due to the different criteria [1].

The hydration of cement-based materials leads to a continuous decrease in the amount of porosity due to the increase in hydration products. The degree of hydration and porosity in a hydration system are essentially correlated. Conventionally, porosity of concrete is measured at mature stages by the MIP method. Powers and Brownyard [2] used a model to relate capillary pores in a cement paste to the degree of hydration and initial water to cement ratio.

Electrical conduction occurs primarily due to ion transport through the pore solution in a cement-based system. It is strongly dependent on both pore solution conductivity and porosity. Electrical measurement methods have been applied to study the microstructural evolution in hydrating cement-based material systems [3–6]. However, the results from conventional electrical measurement are problematic due to the problems of the contact between electrodes and fresh cement, caused by electrochemical reactions and shrinkage gap.

Recently, a non-contact electrical resistivity method (NC-ERM) [7] has been developed to measure the resistivity development of fresh concrete and of the pore solution within the concrete mixes. The NC-ERM eliminates the contact problems between electrodes and surrounding materials in

* Corresponding author. Tel.: +852 23588751; fax: +852 23581534.
*E-mail address:* zongjin@ust.hk (Z. Li).

0008-8846/$ - see front matter © 2007 Elsevier Ltd. All rights reserved.
doi:10.1016/j.cemconres.2007.09.027

conventional set-ups for impedance measurement since there are no electrodes in this set-up. The non-contact electrical resistivity method has been successfully used in the investigation of the hydration process of cement [8], W/C effect of cement paste [9], alkali effect on hydration process of cement [10], and superplasticizer selection [11] in cement pastes.

The feasibility, sensitivity and effectiveness of NC-ERM for monitoring the hydration of cement-based materials have been verified in Ref. [8]. A power law relation between w/c ratio and bulk resistivity at a fixed curing time was found in Ref. [9]. Ref. [10] correlated electrical resistivity development to heat evolution. Two types of superplasticizers were compared by testing the electrical resistivity and fluidity of the pastes and a criterion was established for superplasticizer selection for use in concrete as reported in Ref. [11]. It should be pointed out that previous studies using NC-ERM mainly concentrated on pure cement paste and no attempt was made to interpret the degree of hydration of a concrete from resistivity measurement. However, since more accurate results can now be obtained by NC-ERM for cement paste as well as concrete, it should be possible to obtain the porosity and the degree of hydration of a concrete from the results of NC-ERM. In this study, the effect of fly ash on concrete was investigated. The porosity evolution ($\phi(t)$–$t$) is obtained from the contribution of porosity to the bulk resistivity development in the control sample and the fly ash samples. The derivation of the degree of hydration ($\alpha(t)$) is based on the assumption that the decrease of porosity was related to the volume difference between the hydrates and hydrated cement. The $\alpha(t)$–$t$ curve is compared with the experimental results obtained from thermo-gravimetric analysis and good agreement was observed.

The setting and hardening behavior of fresh concrete with or without fly ash is followed by the characteristic points on the resistivity curves and the effect of fly ash, which modified the kinetics of the hydration, was revealed. It was observed that the linear relationship between compressive strength and degree of hydration revealed by this study extends closer to the original than that reported in the previous studies.

## 2. Raw materials and sample preparation

All tests have been carried out using ordinary Portland cement (ASTM type I), quartz sand with size of 0.6 mm–5 mm and crushed granite with size of 5 mm–10 mm. The density of Portland cement and fly ash (ASTM class F) are 3.15 and 2.2 g/cm$^3$, respectively. The Blaine specific surface area of the cement is 3560 cm$^2$/g. The free lime content is 1.36%. Their chemical compositions are shown in Table 1.

Table 1
The chemical composition of cement and fly ash (%)

| Sample | CaO | $SiO_2$ | $Al_2O_3$ | $Fe_2O_3$ | MgO | $SO_3$ | $K_2O$ | $Na_2O$ | LOI |
|---|---|---|---|---|---|---|---|---|---|
| Cement | 64.37 | 20.53 | 6.20 | 3.23 | 0.82 | 2.47 | 0.43 | 0.17 | 1.78 |
| Fly ash | 3.38 | 49.99 | 37.12 | 3.06 | 0.52 | 0.67 | 0.40 | 0.16 | 3.82 |

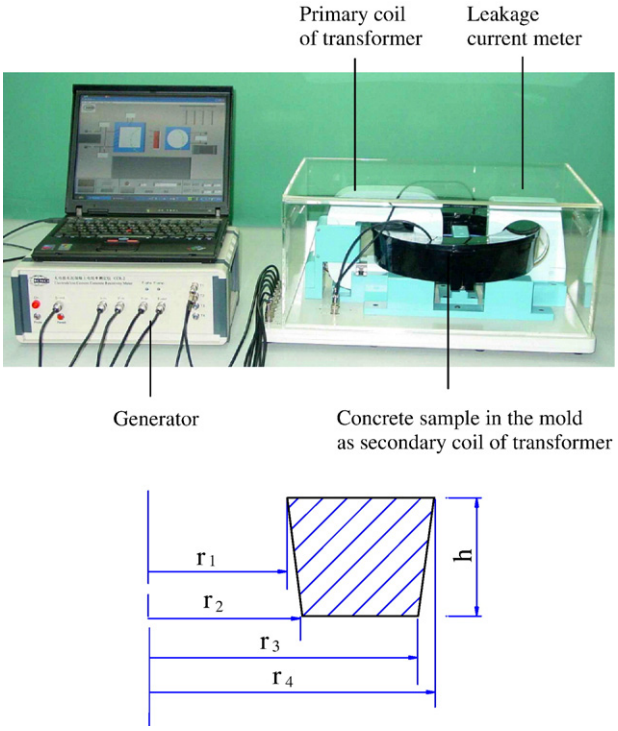


Fig. 1. Pictures of the non-contact electrical resistivity apparatus and mold cross section.

Concrete samples were prepared with a sand/coarse aggregate weight ratio of 0.5 and a total aggregate volume ratio of 60%, at water/binder (cement + fly ash) ratio (w/b) of 0.4. Samples C0.4, C0.4FA25, C0.4FA50 represented concrete with w/b = 0.4, and fly ash replacement by percentages of 0%, 25% and 50%, respectively.

The pore solutions were extracted from another batch of specimens with the same mix proportion through a filter with a vacuum pump at 20, 40, 60, 80, 100, 120, 140, 160 and 180 min and through squeezing by a compression machine [12] at 24 and 48 h. The solution electrical resistivities were denoted as S-C0.4, S-C0.4FA25 and S-C0.4FA50.

The hydrated pastes for thermo-gravimetric analysis were prepared by stopping hydration using acetone at the designated ages and the samples were then dried in a vacuum oven with temperature of 23 °C for 24 h.

## 3. Test methods

### 3.1. Electrical resistivity

The electrical resistivity of the concrete mixes and the pore solution within the mixes was measured by a non-contact electrical resistivity apparatus, as shown in Fig. 1. The transformer principle was adopted in this apparatus. When an AC voltage from the generator was applied to the primary coil of the transformer, a toroidal voltage, $V$, would be inducted in the ring sample that acted as the secondary coil of the transformer. The toroidal current $I$ could be measured by a

leakage current meter and hence the resistance of the concrete could be obtained through $V$ and $I$, based on Ohm's law. For a trapezoidal cross section mould with radius $r_1$, $r_2$, $r_3$ and $r_4$ ($r_1<r_2<r_3<r_4$), as shown in Fig. 1, the formula for the resistivity ($\rho$) was derived as Eq. (1) [13],

$$\rho = \frac{h}{2\pi}\left[-\frac{r_1}{r_2-r_1}\ln\frac{r_2}{r_1}+\ln\frac{r_3}{r_2}+\frac{r_4}{r_4-r_3}\ln\frac{r_4}{r_3}\right]\frac{V}{I} \quad (1)$$

Where $h$ represents the height of the sample.

Each concrete sample was cast into the electrical resistivity mold (1672 $cm^3$ in volume) with a cover preventing water within the sample from evaporation. The measurement of the electrical resistivity was conducted over 48 h at data recording intervals of 1 min, under an ambient temperature of 22±2 °C.

### 3.2. The degree of hydration

Aggregate in concrete is regarded as an inert part without chemical reaction. The degree of hydration of concrete is represented by the reaction of paste fraction. Chemically bonded water is usually used as a measure of the degree of hydration ($\alpha(t)$). Chemically bonded water content in a mix is defined as the mass loss per gram of original binder material between temperatures of 105 °C and 950 °C, measured by thermo-gravimetric analysis. The thermo-gravimetric test was conducted using TGA/DTA 92 from room temperature to 950 °C, with increments of 10 °C/min in $N_2$ environment.

The degree of hydration is calculated from the fraction of chemically bonded water content at time $t$ $\left(\frac{W_n(t)}{C}\right)$ to that of completely hydrated cementitious materials $\left(\frac{W_n}{C_{\text{comp.}}}\text{ or }\frac{W_n}{(C+\text{FA})_{\text{comp.}}}\right)$, as shown in Eq. (2).

$$\alpha(t) = \frac{W_n(t)}{C}\Big/\left(\frac{W_n}{C_{\text{comp.}}}\right) \quad (2)$$

When the ignition loss of the original cement ($L_C$) and fly ash ($L_{FA}$) are considered, the equations are expressed as:

For plain Portland cement sample,

$$\alpha(t) = \left[\frac{W_{105}}{W_{950}}(1-L_C)-1\right]\Big/\frac{W_n}{C_{\text{comp.}}} \quad (3)$$

For fly ash replacement of cement by a ratio of $\beta$, $\beta$=weight of FA/(weight of cement+weight of FA), fly ash (class F) is considered to be unreactive during the examined period, because

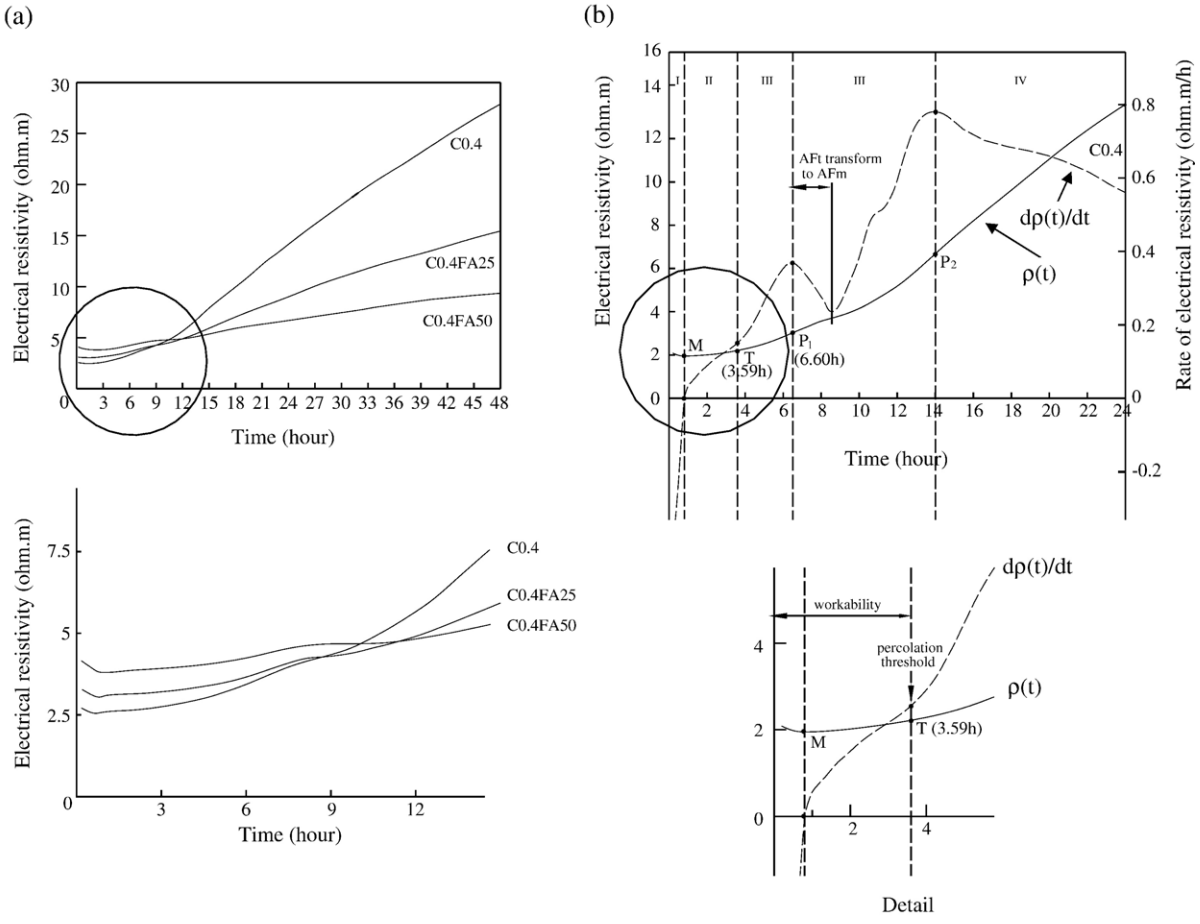


Fig. 2. The bulk electrical resistivity and resistivity rate. (a) Electrical resistivity development $\rho(t)$–$t$. (b) The rate of electrical resistivity development $d\rho(t)/dt$–$t$.

at early age up to 48 h, not much pozzolanic reaction happens [14].

$$\alpha(t) = \left[\frac{W_{105}}{W_{950}}(1-(1-\beta)L_C - \beta L_{FA}) - 1\right] \Big/ \frac{W_n}{(C+FA)_{comp.}} \quad (4)$$

Where $\alpha(t)$: the degree of hydration at time t;

$W_{105}$, $W_{950}$: sample weight at temperature 105 °C and 950 °C at time $t$.

$\frac{W_n}{C_{comp.}}$, $\frac{W_n}{(C+FA)_{comp.}}$: chemical bounded water per gram completely hydrated cementitious material.

The amount of chemically bonded water for completely hydrated cement can be determined based on Bogue's equation [2,15]. A typical value of 0.23 is used for cement [16]. The amount of chemically bonded water for completely hydrated fly ash–cement blend should be slightly lower than that of cement due to the dual effects of fly ash particles provided in the blend, pozzolanic reaction and filler function [17,18].

### 3.3. Mercury intrusion porosimetry (MIP)

The porosity values of the concrete samples at 24 and 48 h were measured using a Micromeritics AutoPore IV 9500 MIP.

### 3.4. Setting time and compressive strength

To evaluate the setting and hardening properties of the concretes, penetration resistance and compressive strength tests were conducted. The setting time of concrete was measured according to ASTM C403. The cubes of size 100×100 mm were prepared and tested at ages of 1 day and 2 days for compressive strength. The samples were prepared with the same mix proportions as those used in the bulk resistivity tests, under the same conditions.

## 4. Experimental results

The bulk electrical resistivity curves with time ($\rho(t)$–$t$) of the concrete mixes are plotted in Fig. 2(a). The differential of the bulk resistivity curve ($d\rho(t)/dt$–$t$) of the control sample C0.4, as an example, is presented in Fig. 2(b). The bulk resistivity development presents the hydration process and the differential gives an assessment of the rate of hydration occurring in the system.

Table 2
The characteristic points on the resistivity curves

| Mix | Point M | | Point T | | Point P1 | | Point P2 | |
|---|---|---|---|---|---|---|---|---|
| | $\rho$ | $t$ | $\rho$ | $t$ | $d\rho/dt$ | $t$ | $d\rho/dt$ | $t$ |
| | (Ω m) | (h) | (Ω m) | (h) | (Ω m/h) | (h) | (Ω m/h) | (h) |
| C0.4 | 2.543 | 0.617 | 2.878 | 3.59 | 0.369 | 6.60 | 0.791 | 14.00 |
| C0.4FA25 | 3.028 | 0.733 | 3.259 | 3.86 | 0.297 | 7.07 | 0.395 | 15.06 |
| C0.4FA50 | 3.787 | 0.917 | 3.960 | 4.08 | 0.233 | 7.56 | 0.216 | 16.02 |

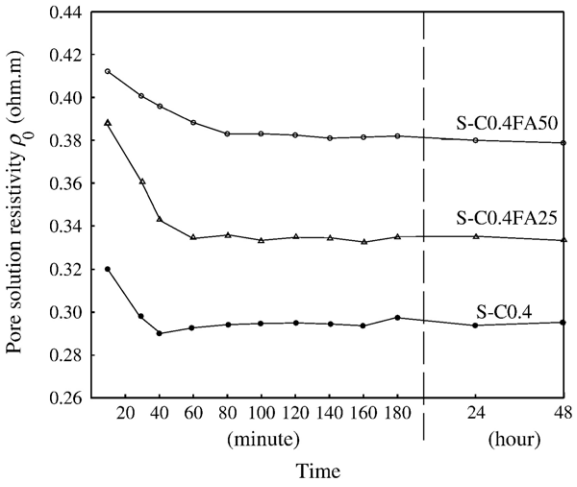


Fig. 3. The electrical resistivity of pore solution $\rho_0(t)$ during the first 48 h.

Two significant results can be seen in Fig. 2. The first one is that the three samples exhibit a similar resistivity/time response. The electrical resistivity $\rho(t)$ drops to the minimum point M and then gradually increases with time at the different rates to points T, P1 and P2, corresponding to turning point, peak 1 and peak 2 on the curve of $d\rho(t)/dt$, respectively. The values of resistivity at point M and the resistivity development rate $d\rho(t)/dt$ of the peak points and the time to reach the characteristic points of each sample are given in Table 2.

The second significant result is that the curves of the fly ash samples show a higher initial electrical resistivity than the control sample due to less soluble ions and a little higher solid fraction in volume in the fly ash samples. However, a slow rise with time in the bulk resistivity of the fly ash samples leads the curves to be overtaken by that of sample C0.4 at a time of 8.4 h

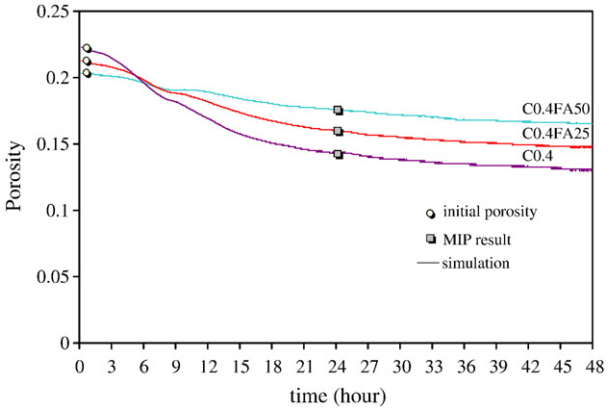


Fig. 4. The porosity development with time for concrete samples during the first 48 h.

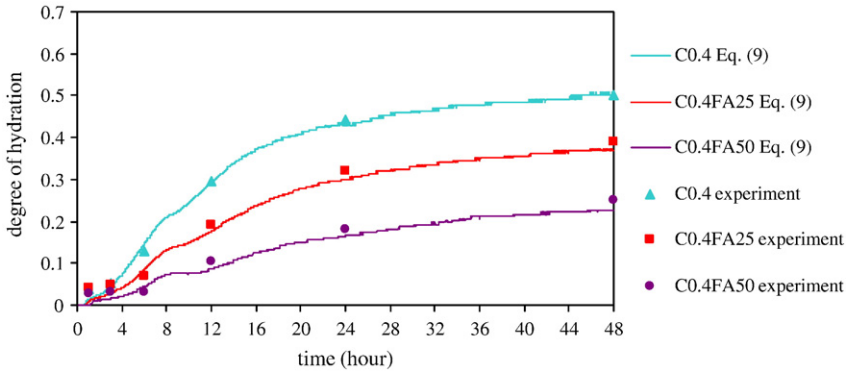


Fig. 5. The degree of hydration with time during the first 48 h.

and 10.1 h, respectively. Meanwhile, the resistivity of sample C0.4FA25 becomes greater than that of sample C0.4FA50 after 11.5 h.

The electrical resistivity development of the pore solution with time ($\rho_0(t)$–$t$) is plotted in Fig. 3. It can be seen that the three curves have similar trends, exhibiting a sharp decrease in resistivity at 40, 60 and 80 min after mixing for samples S-C0.4, S-C0.4FA25 and S-C0.4FA50, followed by a slight fluctuating trend during the rest time up to 48 h, corresponding to the saturation of ion concentration in the pore solution. It can be seen that sample S-C0.4 has the lowest initial $\rho_0$. The $\rho_0$ of sample S-C0.4FA25 is smaller than that of S-C0.4FA50. This trend is consistent with the phenomenon observed in the bulk resistivity development at the early stage for samples C0.4, C0.4FA25 and C0.4FA50. The time corresponding to the inflection point on the curve $\rho_0(t)$–$t$ of each sample is close to that of point M on the curve $\rho(t)$–$t$ of the corresponding concrete mix, suggesting that pore solution resistivity determines the bulk resistivity before reaching that point.

The porosity results of the samples from MIP test and the resistivity model are shown in Fig. 4. The results of the degree of hydration from the thermal analysis are shown by solid dots and the results of the degree of hydration from the porosity simulation are plotted by the curves in Fig. 5. The control sample has a lower porosity and a higher hydration degree compared with the samples with fly ash replacements. The degree of hydration decreases with the increase of the fly ash replacement contents of 25% and 50% at the measured ages.

The test results of setting time and compressive strength at 1 day and 2 days are shown in Table 3.

Table 3
Concrete setting time and compressive strength

| Mix | Setting time (h) | | Compressive strength (MPa) | |
|---|---|---|---|---|
| | Initial | Final | 1 day | 2 days |
| C0.4 | 3.75 | 5.88 | 25.93 | 32.87 |
| C0.4FA25 | 4.03 | 6.43 | 18.55 | 22.31 |
| C0.4FA50 | 4.17 | 7.01 | 10.68 | 13.64 |

## 5. Discussions

### 5.1. Electrical resistivity model and the derived $\phi(t)$–$t$ curve

Conductivity of a concrete is determined mainly by the porosity and conductive ion concentration in the pore solution. From the standpoint of conductivity, concrete can be regarded as a two-component composite material, pore solution and solid phase (aggregate+hydration products+unhydrated binders).

Archie's law [19] reflects the relationship between the resistivity and porosity of rocks saturated with conducting liquid. It can be applied to cement paste for a saturation degree of 100%. A resistivity model presented in Eqs. (5) and (6) was developed from a two-component system to show the relationship of the bulk resistivity evolution $\rho(t)$, pore solution resistivity $\rho_0(t)$ and porosity $\phi(t)$ in concrete [9].

$$\ln\left(\rho(t)\right) = \ln\left(\rho_0(t)\right) - m(t)\ln\left(\phi(t)\right) \tag{5}$$

$$m(t) = m_1 + \frac{\ln\rho(t) - \ln\rho_1}{\ln\rho_2 - \ln\rho_1}\left(m_1 - m_2\right) \tag{6}$$

Where $\rho_1$ and $\rho_2$ are the bulk resistivity values at the initial recording point and age of 1 day. $m$ is a fitting function of time. The $m_1$ and $m_2$ are the $m$ values at the initial point and age of 1 day.

These equations show that the bulk electrical resistivity $\rho(t)$ is a function of the electrical resistivity of the pore solution $\rho_0(t)$ and porosity $\phi(t)$, such that $\rho(t)$ increases with the increase of $\rho_0(t)$ and the decreases of $\phi(t)$.

The main procedures for obtaining the porosity curves $\phi(t)$–$t$ are as follows:

(1) Determine the $m_1$ and $m_2$ values according to the porosity and resistivity values at the two points. The initial porosity is determined by the ratio of the original water volume ratio to the total volume of each constituent in the concrete, and the porosity at 1 day is obtained using MIP, as shown in Table 4.

Table 4
The initial total volume, initial porosity and MIP porosity of the concrete mixes

| Mix | Initial $V_{total}$ ($cm^3$) (1 g binder) | Initial porosity ($\phi_0$) | MIP porosity (1 day) |
|---|---|---|---|
| C0.4 | 1.794 | 0.223 | 0.130 |
| C0.4FA25 | 1.879 | 0.213 | 0.157 |
| C0.4FA50 | 1.965 | 0.204 | 0.179 |

(2) Calculate $m(t)$ according to Eq. (6) using the measured $\rho(t)$.
The $m$ values of samples C0.4, C0.4FA25 and C0.4FA50 range 1.25–2.27, 1.29–2.07 and 1.33–1.83 during the first 48 h, respectively. It is also interesting to note that the change of $m$ values for fly ash blend samples.
It can be seen that $m$ value increases with increasing fly ash content at very early age, it is attributed to the fact that fly ash has a lower specific gravity than cement. Thus, the FA samples have smaller initial porosity and higher initial tortuosity than that of the control sample. However, as the hydration develops, at 48 h after casting, more hydration products develop in a cement system than that develop in a fly ash modified system. This leads to less voids and higher tortuosity in a cement sample. Hence, a higher $m$ value is also reached.

(3) Calculate $\phi(t)$ based on the obtained $\rho(t)$, $\rho_0(t)$ and $m(t)$. The resultant curves $\phi(t)$–$t$ are shown in Fig. 4. It can be seen that the curve $\phi(t)$–$t$ reflects a decrease in porosity. The fly ash samples have a lower decreasing rate of porosity, although the fly ash samples possess a lower initial porosity due to the lower density of the fly ash as compared to that of cement as mentioned earlier. The slow pore-decreasing rate led to the porosity of the fly ash samples being larger than that of the control sample after 4.8 h and 5.6 h, respectively. Subsequently at a time of 6.8 h, the $\phi$ value of sample C0.4FA50 was larger than that of sample C0.4FA25, indicating that fly ash replacement of cement led to a significant dilution effect of cement and reduces the amount of hydrates. Such effect increased with the replacement percentage. It is noted that $\phi(t)$–$t$ dynamically and continuously reflects porosity change in the early hydration system.

### 5.2. The relationship between porosity and hydration degree

Powers–Brownyard proposed a model [2] to describe a hydrated paste, which was assumed to have three components, unhydrated cement, hydration product, and capillary pores. The capillary pores were regarded as the remnants of the initially water filled space in a hydrated cement paste. The porosity of a cementitious paste was dependent on the water cement ratio and the degree of hydration. The degree of hydration could be expressed in terms of water cement ratio and the volume change ratio of pores per gram of cement in the hydration system. At early ages, the capillary pores were considered as main conductive paths and the hydration of class F fly ash is ignored. The porosity was determined by the ratio of the capillary volume $V_{capillary}$ to the total volume of each constituent in the concrete $V_{total}$, as shown in Eq. (7). The degree of hydration could be derived from the porosity obtained by resistivity measurement, as shown in Eq. (8).

$$\phi(t) = \frac{V_{capillary}}{V_{total}} = \left[\frac{W/C}{D_w} - \left(\frac{\alpha(t)}{D_h} - \frac{\alpha(t)}{D_c}\right)\right] \Big/ V_{total} \tag{7}$$

$$\alpha(t) = \left[\frac{W/C}{D_w} - \phi(t)\cdot V_{total}\right] \cdot \frac{D_c D_h}{D_c - D_h} \tag{8}$$

for $D_w = 1.01$ g/cm$^3$, $D_c = 3.15$ g/cm$^3$, $D_h = 1.529$ g/cm$^3$ (based on assuming that 1 unit volume of cement produces 2.06 unit volume of gel) [2], and $W/C = 0.4$,

$$\alpha(t) = 2.971[0.4 - \phi(t)\cdot V_{total}] \tag{9}$$

for sample C0.4, $\alpha(t) = 1.188 - 5.330\phi(t)$
for sample C0.4FA25, $\alpha(t) = 1.188 - 5.583\phi(t)$
for sample C0.4FA50, $\alpha(t) = 1.188 - 5.838\phi(t)$
where $D_w$, $D_c$ and $D_h$ represent the density of the pore solution, cement and hydrates, respectively.

The degree of hydration obtained from the resistivity measurement (using Eq. (9)) is compared with the experimental results of dehydration conducted using the thermo-gravimetric analysis, as shown in Fig. 5. It can be seen in Fig. 5 that the measured results of the degree of hydration are reasonably close to the curves, especially for the control sample. It is noted that experimental results are slightly higher than the results obtained with Eq. (9).

The pores contribution to the conductivity of the mixes is included in the $\phi(t)$–$t$ curves. Therefore, the derived $\alpha(t)$ from $\phi(t)$ can be used as an indicator of the mechanical properties of concrete which are essentially related to porosity within the mix.

### 5.3. Setting and hardening processes

Considering the characteristic points on the resistivity development curves, the resistivity/time response can be divided into 5 regions, designated I, II, III, IV and V, corresponding to dissolution, competition of dissolution–precipitation, setting, hardening and hardening deceleration periods, as shown in Fig. 2(b). A similar observation has been reported and explained in detail in Ref. [9]. Hence, the emphasis here is on the influence of fly ash on the setting and hardening process of concrete.

The bulk electrical resistivity and the rate show a steep increase at point T at the time of 3.59 h for sample C0.4, which is close to its initial setting time 3.75 h, indicating the percolation threshold of the solid phase. The initial setting occurs at times of 3.75 h, 4.03 h and 4.17 h for samples C0.4, C0.4FA25 and C0.4FA50, obtained by ASTM C403 procedures, shown in Table 3, when the degree of hydration is 6.53%, 4.14% and 2.07% (or normalized hydration degree by cement content is 6.53%, 5.52%, 4.14%) respectively. At the final setting times, the degree of hydration is 13.96%, 9.61% and

6.11% (or normalized hydration degree by cement content is 13.96%, 12.81%, and 12.22%), respectively. It is seen that the lower degree of hydration leads to prolonged initial setting for the fly ash samples. The higher the degree of hydration, the earlier the setting time. It suggests that the hydrates content in the samples dominates the setting time and initial strength gain. It can also be seen that the time of occurrence of P1 is very close to the final setting times of samples C0.4, C0.4FA25, and C0.4FA50, which suggests that P1 indicates transition from a setting to a hardening process. The time from point M to point P1 and the resistivity rate at point P1 are related to the fly ash incorporation content, as fly ash prolongs the time from M to P1 and decreases the rate of resistivity development. Fly ash replacement of 25% and 50% causes a retardation of 0.27 h and 0.42 h in the initial setting time, and 0.55 h and 1.13 h in final setting time, respectively. The shift of point P1, caused by fly ash incorporation, is proportional to the change in setting time. The studies show that resistivity development can be used to describe the setting behavior of concrete [20].

After point P1, concrete hydration moves into the hardening period.

Right after P1, the rate of resistivity development ($d\rho(t)/dt$) has a temporary decrease. It could be contributed to phases transform from AF*t* to AF*m* due to consumption of gypsum, releasing conductive ions $Ca^{2+}$ and $SO_4^{2-}$ [21,22]. When the transform reaction between the two phases is in equilibrium, the increase in the degree of cement hydration caused the resistivity rate to increase again until P2 is reached. After point P2, the increase rate of the bulk resistivity decreases, which implies a hardening deceleration.

The characteristic points P1 and P2 on samples C0.4FA25 and C0.4FA50 shift to the right, i.e. it takes a longer time for the fly ash samples to reach the points as shown in Table 2, describing the effect of fly ash addition in delaying each hydration stage. The delayed setting and hardening stages of the fly ash samples can be attributed to less cement in the fly ash samples.

The inclusions of class F fly ash in the binder results in a decrease of strength development (see Table 3) in comparison to the control mix, particularly for 50% fly ash incorporation. The concretes with fly ash have lower compressive strengths. Higher dosages of fly ash lead to lower hydration degrees and lower compressive strengths, which is the same trend as that in the bulk resistivity evolution.

### *5.4. The relationship between the degree of hydration and compressive strength*

Strength development in the concrete mixes relies on the increase of the hydration degree or the decrease of porosity. The correlation of compressive strength and the degree of hydration is plotted in Fig. 6. It can be seen that the relationship exhibits a linear trend, and is independent of the fly ash incorporation. The differences of strength among samples C0.4, C0.4FA25 and C0.4FA50 are consistent with the differences in the degree of hydration. It should be pointed that a similar linear relationship between compressive strength and the degree of hydration has been reported in Ref. [2]. However, the intercept that appeared in current research is much close to the origin, implying that strength gain is strongly dependent on hydration. The retarding effect of fly ash on hydration process appears in the resistivity parameters and the porosity, which form the basis for deriving the degree of hydration.

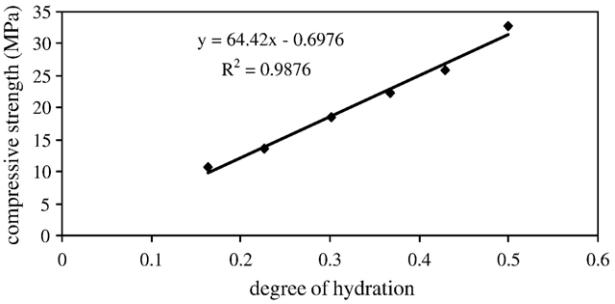


Fig. 6. The relationship of the degree of hydration and compressive strength at 1 day and 2 days.

It can be concluded that the curves $\alpha(t)$–$t$ dynamically reflect the internal microstructure development and strength development in cement-based materials. The degree of hydration is a direct indicator of strength and the resistivity in return is an indirect measure of its strength.

## 6. Conclusions

The main conclusions can be drawn as follows:

1. The characteristic points on $\rho(t)$–$t$ reflect the transition processes during hydration of concrete. The lowest point M on the $\rho(t)$–$t$ curve shows that the dissolution process reaches the supersaturation point of the solution. The first peak point P1 on $d\rho(t)/dt$–$t$ exhibits that the time occurring is related to final setting of concrete mixes.
2. The $\alpha(t)$–$t$ is obtained by electrical resistivity measurement and shows a good agreement with the experimental results of thermo-gravimetric analysis. The $\alpha(t)$–$t$ variation exhibited in fly ash samples shows how much fly ash retards cement hydration in the early stage. The larger the amount of fly ash incorporation, the stronger the retarding effect.
3. The linear relationship between the degree of hydration and compressive strength shows that the degree of hydration is a direct indicator of compressive strength and is independent of fly ash incorporation. The curve $\alpha(t)$–$t$ developed from electrical resistivity measurement reflects the hydration kinetics of fresh concrete.

## Acknowledgement

The financial support from the Hong Kong Research Grant Council under grant number HKUST 6272/03E and from NSFC50578142 is gratefully acknowledged.

## References

[1] G. Ye, Experimental study and numerical simulation of the development of microstructure and permeability of cementitious materials, PhD Thesis. Delft University of Technology, Delft, 2003.

[2] T.C. Powers, T.L. Brownyard, Studies of the physical properties of hardened Portland cement paste, Research Laboratories of the Portland Cement Association, Chicago, Bulletin, vol. 22, 1948.
[3] W.J. McCarter, T.M. Chrisp, G. Starrs, J. Blewett, Characterization and monitoring of cement-based systems using intrinsic electrical property measurements, Cement and Concrete Research 33 (2) (2003) 197–206.
[4] B.J. Christensen, R.T. Coverdale, R.A. Olson, et al., Impedance spectroscopy of hydrating cement-based materials: measurement, Interpretation, and application, Journal of the American Ceramic Society 77 (11) (1994) 2789–2804.
[5] Z.Z. Xu, P. Gu, P. Xie, J.J. Beaudoin, Application of A.C. impedance techniques in studies of porous cementitious materials, Cement and Concrete Research 23 (4) (1993) 853–862.
[6] H.W. Whittington, J. McCart, M.C. Forde, The conduction of electricity through concrete, Magazine of Concrete Research 33 (114) (1981) 48–60.
[7] Z. Li, W. Li, Non-contacting method for resistivity measurement of concrete specimen. US Patent (US 6639401).
[8] Z. Li, X. Wei, W. Li, Preliminary interpretation of Portland cement hydration process using resistivity measurements, ACI Materials Journal 100 (3) (2003) 253–257.
[9] X. Wei, Z. Li, Early hydration process of Portland cement paste by electrical measurement, Journal of Materials in Civil Engineering 18 (1) (2006) 99–105.
[10] Z. He, Z. Li, Non-contact resistivity measurement for characterisation of the hydration process of cement-paste with excess alkali, Advances in Cement Research 16 (1) (2004) 29–34.
[11] L. Xiao, Z. Li, X. Wei, Selection of superplasticizer in concrete mix design by measuring the early electrical resistivities of pastes, Cement and Concrete Composites 29 (5) (2007) 350–356.
[12] N.R. Buenfeld, J.B. Newman, Examination of three methods for studying ion diffusion in cement pastes, mortars, and concrete, Materials and Structures 20 (1987) 3–10.
[13] X. Wei, Z. Li, Non-contacting resistivity measurement for hydration of cement-based materials [A], in: R.K. Dhir, M.D. Newlands, M.J. Mccarthy (Eds.), Role of cement science in sustainable development, Thomas Telford Ltd., London, 2003, pp. 81–92.
[14] L. Xiao, Z. Li, Evaluation of activity of mineral admixtures at early age and long term in cementitious system, 6th International Symposium on Cement & Concrete (6th ISCC), 2006.
[15] L. Molina, On predicting the influence of curing conditions on the degree of hydration, CBI Report 5:92, Swedish Cement and concrete research institute, Stockholm, Sweden, 1992.
[16] H.F.W. Taylor, Cement Chemistry, 2nd eds., T. Telford, London, 1997, p. 198.
[17] H.F.W. Taylor, K. Mohan, G.K. Moir, Analytical study of pure and extended Portland cement pastes: I, fly ash– and slag–cement pastes, Journal of the American Ceramic Society 68 (12) (1985) 685–690.
[18] H.F.W. Taylor, K. Mohan, G.K. Moir, Analytical study of pure and extended Portland cement pastes: II, pure Portland cement pastes, Journal of the American Ceramic Society 68 (12) (1985) 680–685.
[19] G.E. Archie, The electrical resistivity log as an aid in determining some reservoir characteristics, Transactions of the AIME 146 (1942) 54–62.
[20] Z. Li, L. Xiao, X. Wei, Determination of concrete setting time using electrical resistivity measurement. Journal of Materials in Civil Engineering 19 (5) (2007) 423–427.
[21] S.A. Abo El-Enein, M.F. Kotkata, G.B. Hanna, et al., Electrical resistivity of concrete containing silica fume, Cement and Concrete Research 25 (8) (1995) 1615–1620.
[22] L. Xiao, Interpretation of hydration process of concrete based on electrical resistivity measurement, PhD Thesis, Hong Kong University of Science and Technology, Hong Kong, 2007.